

MIT Open Access Articles

Heterogeneity in mouse spasmolytic polypeptide-expressing metaplasia lineages identifies markers of metaplastic progression

The MIT Faculty has made this article openly available. **Please share** how this access benefits you. Your story matters.

Citation: Weis, V. G. et al. "Heterogeneity in Mouse Spasmolytic Polypeptide-expressing Metaplasia Lineages Identifies Markers of Metaplastic Progression." *Gut* (2012): p.1-10. Web. ©2012 BMJ Publishing Group Ltd & British Society of Gastroenterology.

As Published: <http://dx.doi.org/10.1136/gutjnl-2012-302401>

Publisher: BMJ Publishing Group

Persistent URL: <http://hdl.handle.net/1721.1/74663>

Version: Final published version: final published article, as it appeared in a journal, conference proceedings, or other formally published context

Terms of Use: Article is made available in accordance with the publisher's policy and may be subject to US copyright law. Please refer to the publisher's site for terms of use.



ORIGINAL ARTICLE

Heterogeneity in mouse spasmolytic polypeptide-expressing metaplasia lineages identifies markers of metaplastic progression

Victoria G Weis,¹ Josane F Sousa,¹ Bonnie J LaFleur,² Ki Taek Nam,¹ Jared A Weis,³ Paul E Finke,⁴ Nadia A Ameen,⁵ James G Fox,⁶ James R Goldenring¹

► Additional materials are published online only. To view these files please visit the journal online (<http://dx.doi.org/10.1136/gutjnl-2012-302401/content/early/recent>).

¹Nashville VA Medical Center and the Departments of Surgery and Cell and Developmental Biology, Epithelial Biology Center, Vanderbilt University School of Medicine, Nashville, Tennessee, USA

²Division of Epidemiology and Biostatistics, University of Arizona, Tucson, Arizona, USA

³Department of Biomedical Engineering, Vanderbilt University, Nashville, Tennessee, USA

⁴Department of Medicinal Chemistry, Merck Research Laboratories, Rahway, New Jersey, USA

⁵Departments of Pediatrics/Gastroenterology and Hepatology, Yale University School of Medicine, New Haven, Connecticut, USA

⁶Division of Comparative Medicine, Massachusetts Institute of Technology, Cambridge, Massachusetts, USA

Correspondence to

Dr James R Goldenring, Vanderbilt University School of Medicine, Epithelial Biology Center, 10435G MRBIV, 2213 Garland Avenue, Nashville, TN 37232-2733, USA; jim.goldenring@vanderbilt.edu

Revised 24 May 2012
Accepted 27 May 2012

ABSTRACT

Objectives Spasmolytic polypeptide-expressing metaplasia (SPEM) develops as a preneoplastic lesion in the stomachs of mice and humans after parietal cell loss. To identify the commonalities and differences between phenotypic SPEM lineages, SPEM were studied from three different mouse models of parietal cell loss: with chronic inflammation with *Helicobacter felis* infection; with acute inflammation with L635 treatment; and without inflammation following DMP-777 treatment.

Design RNA transcripts from laser capture microdissected normal chief cells and SPEM lineages were compared using gene microarray. Alterations in transcripts were validated by quantitative real-time PCR. Clusterin and cystic fibrosis transmembrane conductance regulator (CFTR) were selected for immunohistochemical analysis in all mouse models as well as in human SPEM, intestinal metaplasia and gastric cancer.

Results Transcript expression patterns demonstrated differences among the phenotypic SPEM models. Clusterin expression was significantly upregulated in all three mouse SPEM models as well as in human SPEM. The highest clusterin expression in human gastric cancers correlated with poor survival. Conversely, CFTR expression was upregulated only in SPEM with inflammation in mice. In humans, intestinal metaplasia, but not SPEM, expressed CFTR.

Conclusions While markers such as clusterin are expressed in all phenotypic SPEM lineages, distinct patterns of upregulated genes including CFTR are present in murine metaplasia associated with inflammation, indicative of progression of metaplasia towards a more intestinalised metaplastic phenotype.

INTRODUCTION

Helicobacter pylori infection is the major predisposing factor for human gastric cancer.¹ In humans, *H pylori* infection causes a disruption in the gastric homeostasis by inducing prominent chronic inflammation and loss of parietal cells. The loss of parietal cells leads to two distinct types of mucous cell metaplasia: intestinal metaplasia and spasmolytic polypeptide-expressing metaplasia (SPEM). Increasing evidence in humans and rodent models suggests that intestinal metaplasia develops in the presence of pre-existing SPEM, supporting the concept that SPEM is a neoplastic precursor in the carcinogenesis cascade.²⁻⁴

Significance of this study**What is already known on this subject?**

- SPEM and intestinal metaplasia are both associated with gastric cancer.
- While parietal cell loss in mice results in the emergence of SPEM from transdifferentiation of chief cells, inflammation is necessary for SPEM to progress to dysplasia.
- *Helicobacter felis* infection in mice results in SPEM that progresses directly to dysplasia without ever developing phenotypic intestinal metaplasia.

What are the new findings?

- Phenotypically similar SPEM lineages from different mouse models of induction possess both commonalities and differences in their expression profiles.
- Clusterin is a marker of all SPEM lineages in mice and humans and is a marker of poor prognosis for gastric adenocarcinomas.
- CFTR is expressed in SPEM associated with inflammation in the mouse, but only in intestinal metaplasia in humans.
- In mice, SPEM emerges after the loss of parietal cells but progresses in the presence of inflammation to a more advanced SPEM with intestinal characteristics analogous to the progression of SPEM to intestinal metaplasia in humans.

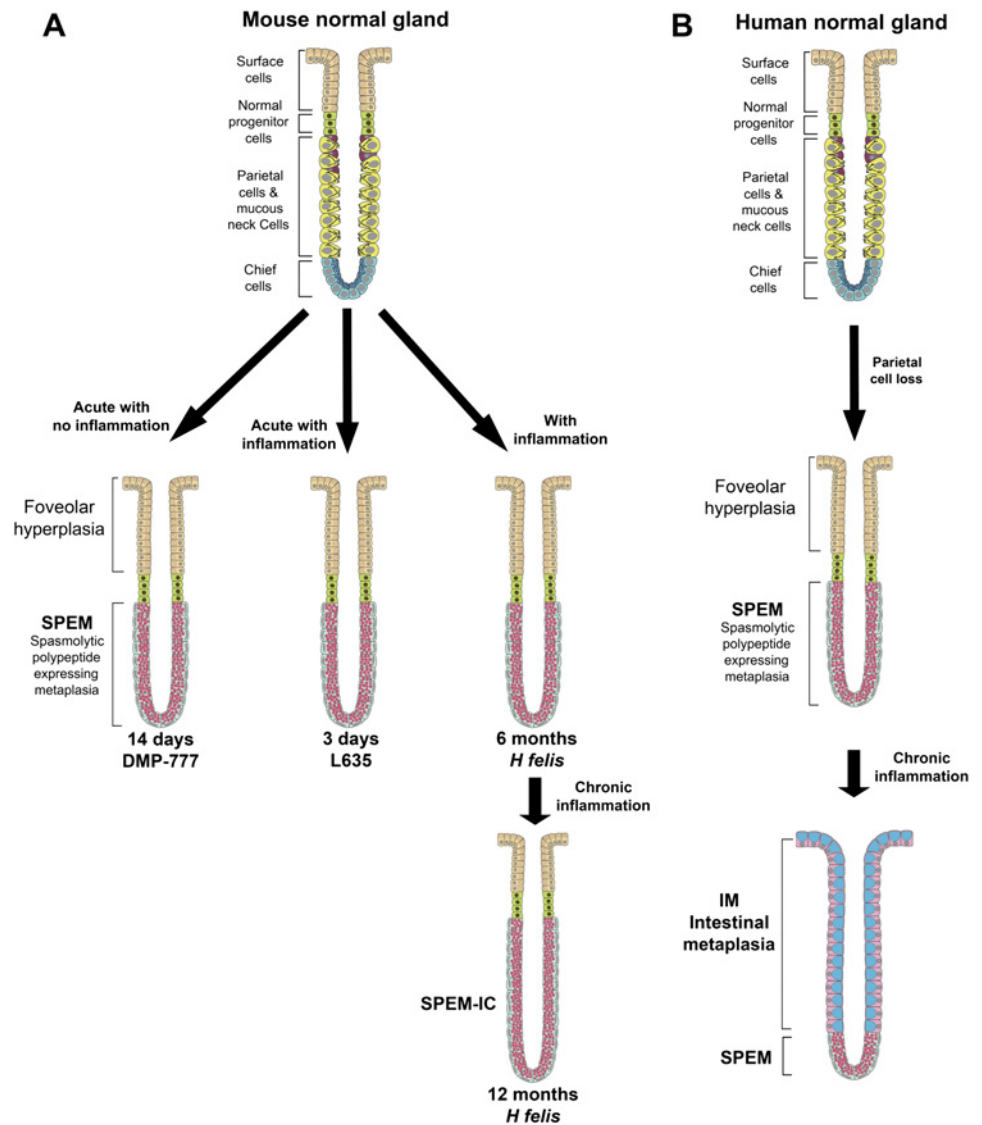
How might it impact on clinical practice in the foreseeable future?

- Recognition of the heterogeneity of phenotypic metaplastic lineages suggests that detailed molecular characterisation may classify lesions with a greater risk of progression to dysplasia and cancer.

Chronic *Helicobacter felis* infection in mice is a critical model for *H pylori* infection in humans. After 6 months of *H felis* infection, significant parietal cell loss accompanied by inflammation leads to the emergence of a proliferative SPEM lineage derived almost completely from transdifferentiated chief cells⁵ (figure 1A). SPEM progresses to dysplasia after 1 year of infection without developing phenotypic intestinal metaplasia.^{6,7} All present evidence thus indicates that SPEM is the direct precursor to

Gastric cancer

Figure 1 Models of phenotypic spasmolytic polypeptide-expressing metaplasia (SPEM) in mice and of metaplastic progression in humans. (A) The three mouse models used in these investigations all display phenotypic SPEM. DMP-777 administration is an acute model of parietal cell loss that results in SPEM without inflammation. L635 administration is also an acute model of SPEM; however, L635-induced SPEM is accompanied by prominent inflammation. *H felis* infection is a SPEM model phenotypically similar to L635 but with chronic inflammation. *H felis* infection induces SPEM at 6 months but progresses with chronic inflammation to acquire intestinal characteristics. (B) In humans, loss of parietal cells leads to the emergence of SPEM. Intestinal metaplasia (IM) arises from SPEM under the influences of chronic inflammation. This figure is produced in colour in the online journal—please visit the website to view the colour figure.



dysplasia in *H felis*-infected mice. A mouse model of acute oxyntic atrophy using the parietal cell-specific protonophore, DMP-777, allows for the separation of the roles of parietal cell loss and inflammation in the initiation of SPEM (figure 1A).^{8,9} Oral gavage administration of DMP-777 for 14 days induces SPEM as a direct result of parietal cell loss. However, DMP-777 also inhibits any inflammatory response because of its ability to inhibit neutrophil elastase potentially resulting in SPEM, which is less proliferative.^{8,9} Moreover, DMP-777-induced SPEM contains two distinct component lineages: transdifferentiated chief cells at the gland bases and mucous neck cell hyperplasia in the neck region.⁵ Even after a year of DMP-777 administration, SPEM fails to progress to dysplasia.⁸ The DMP-777 model thus shows that parietal cell loss is sufficient for SPEM initiation, but inflammation is necessary for the progression of SPEM to dysplasia. In contrast, acute administration of L635, a protonophore analogue of DMP-777 that lacks elastase inhibition results in a prominent inflammatory response and induces a SPEM lineage phenotypically similar to *H felis* infection (figure 1A).⁵ Analysis of the progression to dysplasia with chronic administration of L635 is not currently feasible due to limited supplies of the drug. These results have led to the concept that transdifferentiation of chief cells to SPEM is common to all SPEM lineages, but inflammatory cells drive the evolution of metaplasia towards a more proliferative lineage and

later to dysplasia. However, no studies have investigated differences in expression among phenotypic SPEM lineages.

To investigate the different phenotypic SPEM lineages, we have compared transcriptional expression profiles for micro-dissected chief cells from untreated C57BL/6 mice with micro-dissected SPEM cells from mice after 6–12 months of *H felis* infection, 3 days of L635 administration, or 14 days of DMP-777 administration. *Wfdc2* (HE4), the previously reported SPEM and intestinal metaplasia marker,¹⁰ and clusterin (*Clu*) were up-regulated in all SPEM models. Cystic fibrosis transmembrane conductance regulator (*CFTR*), was not found in normal gastric mucosa or SPEM without inflammation, but was up-regulated in inflammatory SPEM. In humans, *CFTR* was expressed only in intestinal metaplasia, but not in normal mucosa or SPEM. Together, these findings indicate that distinct heterogeneity is present in different animal models of phenotypic SPEM, and that SPEM in the context of inflammation acquires the expression of intestinalising transcripts that resemble features of intestinal metaplasia in humans.

METHODS

Gene microarray analysis

DMP-777 or L635 was administered by oral gavage to groups of six 7-month-old C57BL/6 male mice. Another group of six mice

(two males and four females) were *H felis* infected for 6–12 months. Untreated C57BL/6 male mice were used as controls. Chief cells from control mice or SPEM lineages at the base of glands from treated mice were laser capture microdissected from frozen sections of fundic stomach. Total RNA was isolated from microdissected cells with the Picopure RNA isolation kit (Arcturus, Mountain View, California, USA). The Nugen WT Pico kit (San Carlos, California, USA) was used to reverse transcribe and amplify 25 ng of total RNA for each sample. Fragmented and labelled samples were hybridised to Affymetrix mouse gene 1.0ST arrays (Santa Clara, California, USA) using standard Affymetrix protocols. Statistical analysis is described in the supplementary material (available online only). The generated candidate lists were then compared with each other to create the comparison categories (table 1 and supplementary tables 1–5, available online only).

Quantitative real-time PCR

Total RNA was used for analysis of relative expression as previously reported⁵ and summarised in the supplementary material (available online only). The specific primer sequences and concentrations are listed in supplementary table 6 (available online only).

Immunohistochemistry

Primary and secondary antibodies are listed in the supplementary material (available online only). Sections were analysed using a Zeiss Axiophot microscope equipped with an Axiovision digital imaging system (Zeiss, Jena GmbH, Germany) or an Olympus FV1000 confocal microscope (Olympus, Tokyo, Japan) and tissue arrays were analysed using the Ariol SL-50 automated slide scanner (Genetix, San Jose, California, USA).

RESULTS

Gene microarray analysis of phenotypic SPEM lineages with and without inflammation

To compare the expression profiles of SPEM lineages arising in different milieus, we used laser capture microdissection to isolate chief cells from control untreated mice and SPEM cells at the bases of glands from mice treated with DMP-777, L635, or *H felis* infection. These SPEM models were selected based on their distinct characteristics such as length of treatment (acute vs chronic) and progression to dysplasia (presence vs absence of inflammation; figure 1A), so that the commonalities and differences among the different phenotypic SPEM lineages could be analysed. Levels of isolated messenger RNA transcripts from the microdissected cells were measured with Affymetrix gene microarrays. Five comparison categories were established based on the SPEM model characteristics (as mentioned above) to analyse upregulated transcripts associated with either the emergence or progression of SPEM (listed in table 1 with heat maps of each group shown in supplementary figure 1, available online only). The pan-SPEM and acute SPEM categories focus on transcripts upregulated with the induction of SPEM. Transcripts upregulated in all SPEM lineages compared with chief cells are markers indicative of the initiation of SPEM (pan-SPEM). Eight transcripts were upregulated in pan-SPEM including the secreted glycoprotein, Clu, and the previously reported SPEM marker, whey acidic protein 4 disulfide core domain 2 (Wfdc2, also known as HE4).¹⁰ In the previous study, we identified HE4 as a marker of SPEM and intestinal metaplasia that was not found in the normal stomach.¹⁰ The acute SPEM comparison, consisting of transcripts increased in acute SPEM lineages (DMP-777 and L635-induced SPEM) versus chief cells, revealed tran-

Table 1 Upregulated transcripts in three mouse models of SPEM

	Chief cells	DMP-777	L635	<i>H felis</i>
I. Pan-SPEM				
Ccnb2*	•	2.01	2.55	1.82
Cenpk*	•	1.35	2.60	1.27
Clu	•	1.04	1.58	1.38
Cxcl17	•	1.50	1.81	1.56
Sifn9	•	1.33	2.18	1.33
Top2a*	•	1.95	2.92	2.11
Traf4	•	1.75	2.18	1.59
Wfdc2	•	1.62	1.50	3.12
II. Acute SPEM				
Chek2	•	1.23	1.42	
Figl1	•	1.19	1.93	
Mmp12	•	1.91	2.79	
Tmem48	•	0.78	1.76	
Ube2c	•	1.61	2.88	
III. SPEM with inflammation				
Cftr*	•		3.14	5.78
Ctss*	•		1.24	2.03
Dmbt1*	•		2.72	2.77
Etv5	•		2.01	3.13
Gpx2*	•		2.36	3.00
Mad2l1*	•		2.12	1.78
Prom1*	•		0.73	1.44
IV. Specific to SPEM with inflammation				
Arhgap9		•	0.84	0.77
Cd14		•	1.53	2.72
Ceacam10		•	0.36	2.17
Glipr1		•	0.98	0.84
Gpr171		•	1.89	2.17
Ly6a		•	0.75	1.26
Lyz2		•	2.53	1.97
Ms4a6b		•	1.45	1.94
Ms4a6c		•	2.13	2.03
Tyrobp		•	1.47	1.15
V. SPEM with chronic inflammation				
Casp1*	–4.10	–4.45	–4.32	•
Ceacam1*	–3.44	–3.05	–2.28	•
Gpa33*	–2.93	–2.74	–3.60	•
Il18r1*	–3.09	–1.66	–1.99	•
Itga2*	–2.87	–2.61	–2.81	•
Muc4*	–3.74	–3.34	–3.77	•
Pigr*	–5.37	–3.29	–3.16	•
Vil1*	–2.59	–2.26	–2.60	•

Normal chief cells and spasmodic polypeptide-expressing metaplasia (SPEM) lineages from three SPEM models were compared by gene microarray (six mice per group). Five comparison categories were established: pan-SPEM (I), acute SPEM (II), SPEM with inflammation (III), specific to SPEM with inflammation (IV) and SPEM with chronic inflammation (V).

The linear fold change in each sample group is listed compared with the column marked with a bullet point (•).

In categories I, II and III fold changes are upregulated compared with chief cells. Category IV changes are compared with DMP-777.

In category V listed transcripts are upregulated in *H felis* compared with each of the other groups; thus fold changes are shown as relative downregulation in the respective groups.

*Transcripts previously found upregulated in human metaplasias of the stomach.¹¹

scripts that initially increase in SPEM induction, but decrease in chronic SPEM lineages. Acute SPEM identified five additional transcripts upregulated in the initiation of SPEM (table 1), which included fidgetin-like 1 (Figl1), a transcript previously reported as upregulated in gastrin-deficient mice treated with DMP-777.¹⁰

Because previous studies have indicated that SPEM cannot progress to dysplasia in the absence of inflammation,^{8, 12} transcripts putatively involved in the progression of SPEM were identified with comparisons focusing on SPEM accompanied by

inflammation (L635 and *H felis*-induced SPEM). Transcripts increased in L635 and *H felis*-induced SPEM versus chief cells are listed as 'SPEM with inflammation', whereas the comparison of inflammatory SPEM with non-inflammatory SPEM (DMP-777-induced SPEM) identified 'specific to SPEM with inflammation' transcripts. The 'SPEM with chronic inflammation' category compares *H felis*-induced SPEM with acute SPEM models (with and without inflammation) and chief cells. Ten transcripts were upregulated in the specific to SPEM with inflammation comparison. The SPEM with inflammation and SPEM with chronic inflammation categories yielded numerous upregulated transcripts (43 and 131, respectively; selected transcripts are listed in table 1). Pathway analysis of the comparison categories only identified an increase in interferon γ -associated genes in SPEM with chronic inflammation (supplementary figure 2, available online only). As a whole, these gene microarray studies demonstrated that phenotypic SPEM lineages did indeed demonstrate distinct differences in transcript expression.

To narrow the lists for further investigation, we compared the upregulated transcripts with transcripts previously reported as upregulated in microdissected human metaplasias of the stomach (SPEM or intestinal metaplasia) by gene microarray¹¹ (table 1). Nine transcripts from SPEM with inflammation, including the chloride transporter, CFTR homologue, were also upregulated in human metaplasia, while 17 common transcripts were found for SPEM with chronic inflammation. Only three other transcripts from the other comparison categories, topoisomerase (DNA) II α (Top2a), cyclin B2 and centromere protein K, were also upregulated in the human metaplasia microarrays. We thus found considerable overlap in transcripts associated with SPEM with inflammation in mice and those associated with metaplasias in humans.

Quantitative PCR analysis of upregulated transcripts

Quantitative real-time PCR (qRT-PCR) was used to evaluate further selected upregulated transcripts from each of the comparison categories (figure 2 and supplementary figures 2–7, available online only). *H felis*-induced SPEM was divided into two time points (6 and 12 months) to distinguish between the earlier stages of SPEM and chronic SPEM. In these studies, regions of whole gastric fundus were used for qRT-PCR, rather than microdissected samples. While this approach failed to validate all transcripts from the categories, it allowed for analysis of and insight into upregulation on a more global scale. The poorly understood gene, schlafen 9 (Sln9), from the pan-SPEM category was significantly upregulated in all SPEM models versus normal gastric mucosa (figure 2A). HE4 expression showed an increasing trend in all SPEM models, but failed to reach statistical significance in all individual comparisons. Clusterin was significantly upregulated in acute SPEM models, and there was a trend towards upregulation in 12-month *H felis* infection-induced SPEM (figure 2A). All five acute SPEM transcripts were significantly increased in DMP-777 and L635-induced SPEM versus normal mucosa (figure 2B and supplementary figure 4, available online only). The six transcripts in SPEM with inflammation that were upregulated in human metaplasias of the stomach were tested along with a selected transcript, ets variant gene 5 (ETV5), which was the only transcription factor found in the category (figure 2C and supplementary figure 5, available online only). Many of the transcripts, including CFTR and ETV5, were validated as significantly upregulated in SPEM with inflammation compared with normal mucosa. CFTR expression increased over 100-fold in 12-month *H felis* infection-induced SPEM. Notably, ETV5 was significantly upregulated in L635 and 6-month *H felis*

infection-induced SPEM, but decreased to near normal levels after 12 months of *H felis* infection. Similar to pan-SPEM transcripts, not all of the specific to SPEM with inflammation transcripts followed the trend found in the microarray data with statistical significance (figure 2D and supplementary figure 6, available online only). Expression of carcinoembryonic antigen-related cell adhesion molecule 10 (Ceacam10) and TYRO protein tyrosine kinase binding protein (Tyrobp) expression was significantly increased in inflammatory SPEM models compared with the non-inflammatory SPEM model. While others such as glioma pathogenesis-related 1 (Glipr1) and the two members of the membrane-spanning 4-domains subfamily A, member 6B and member 6C (Ms4a6b and Ms4a6c), followed the trend, but did not achieve statistical significance. Five transcripts from SPEM with chronic inflammation that were also upregulated in human metaplasias of the stomach⁹ were selected for qRT-PCR analysis (figure 2E and supplementary figure 7, available online only). Four of these transcripts, including villin 1 (Vil1), were significantly upregulated in the 12-month *H felis* infection-induced SPEM model compared with the other sample groups (acute SPEM models and control). Together, these results provide a consistent profile of the alterations in the expression of the transcripts in each comparison category, and thus classify gene expression characteristics of SPEM with and without inflammatory influence.

Clusterin expression is increased in all SPEM lineages

Based on antibody availability, we selected Clu from the Pan-SPEM category to investigate protein expression profiles of the induction of SPEM. Clusterin is a ubiquitously expressed secreted glycoprotein thought to be involved in a variety of cellular processes such as tissue remodelling, differentiation, cytoprotection and anti-apoptosis.^{13–18} In untreated mice, Clu staining was observed at low levels only in cells in the isthmus of the oxyntic glands (figure 3). Some Clu-positive cells co-labelled with the first few TFF2-expressing mucous neck cells. In all SPEM models, Clu was strongly expressed throughout the SPEM lineages (figure 3). Differences in the upregulation of Clu mRNA versus detectable protein suggest that Clu mRNA is processed differently between the SPEM lineages. Together, these results demonstrate that Clu protein expression is a marker of SPEM regardless of the causation or surrounding milieu of chief cell transdifferentiation to SPEM.

Upregulation of CFTR expression is observed only in SPEM with inflammation

To investigate possible markers for the progression of SPEM lineages, we examined the expression of CFTR, the most upregulated transcript in SPEM with inflammation as detected by qRT-PCR. CFTR is an ATP-gated chloride channel, which is found on the apical membrane of epithelial cells including intestinal crypt cells.¹⁹ CFTR was not detected in the normal gastric fundus (figure 4) confirming previous investigations.²⁰ Although CFTR mRNA was increased in all SPEM lineages, DMP-777-induced SPEM lineages lacked detectable CFTR protein expression. However, expression of CFTR protein was observed in the apical membranes of the inflammatory SPEM lineages induced by either L635 administration or *H felis* infection, which both have large increases in CFTR mRNA expression (figure 4). These results show that CFTR is a marker of advanced proliferative SPEM.

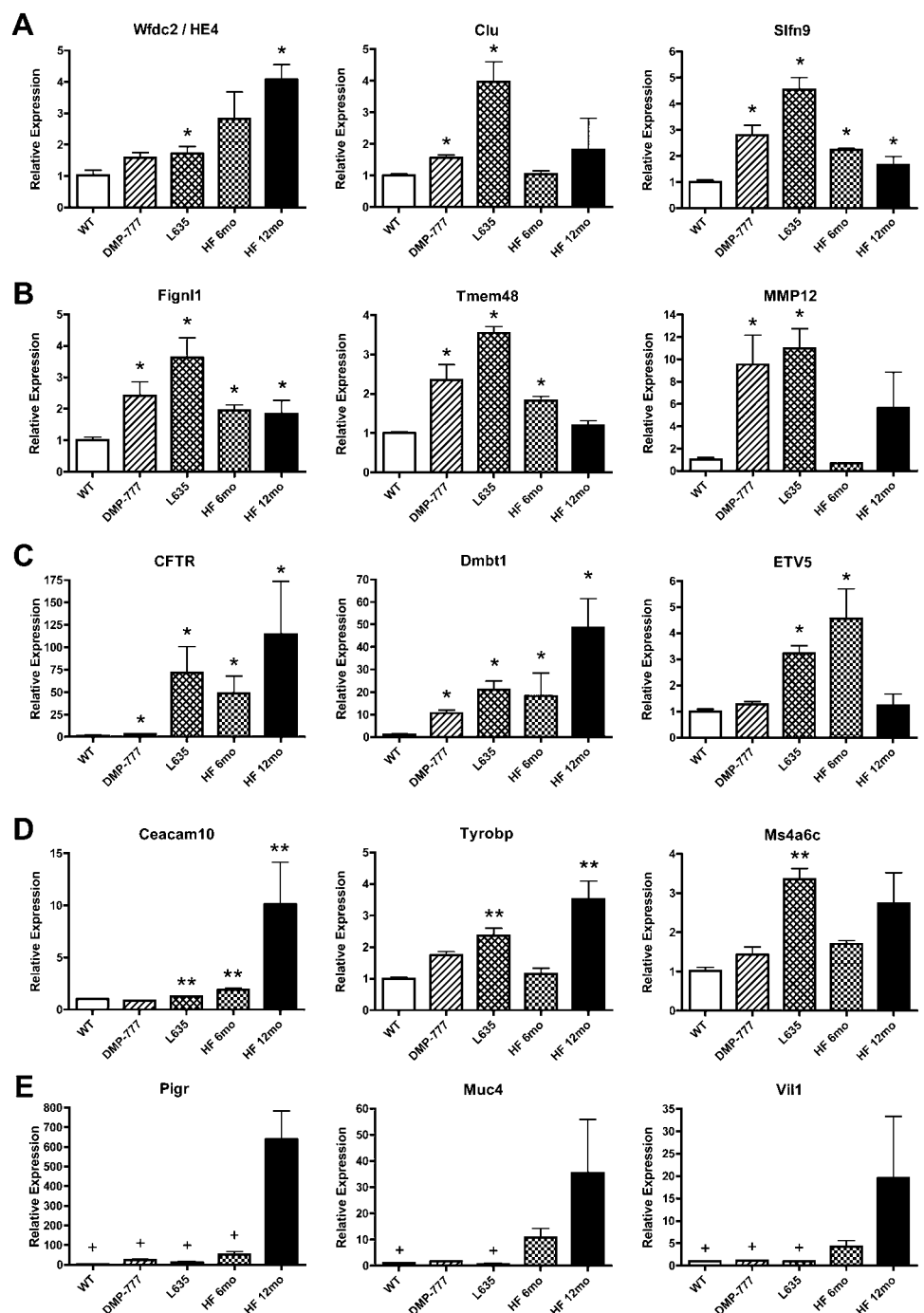
Clusterin and CFTR expression in human metaplasias of the stomach and gastric cancer

Based on the murine data, we examined the expression of Clu and CFTR in human gastric tissues. In normal human gastric

mucosa, Clu was detected in the isthmus region of fundic glands (figure 5A). Some dual-labelling with TFF2 was observed in cells near the upper neck region of oxyntic glands, similar to our observations in mice. In metaplasias of the stomach, Clu had a granular pattern throughout SPEM glands, but was limited to a few cells at the bases of glands when detected in intestinal metaplasia (figure 5B). These Clu-positive intestinal metaplasia cells did not express TFF2. In a tissue array of metaplasias from the human gastric fundus, 90% of cores with SPEM and 46% with intestinal metaplasia (18/20 and 5/11, respectively) were positive for the respective Clu staining patterns. In a small cohort of gastric adenocarcinomas collected at Vanderbilt, Clu was expressed in 56.5% of cancers (9/16 intestinal type and 4/7 diffuse type). A second cohort of 450 Korean patient samples, predominantly early stage cancers, was used to assess Clu as

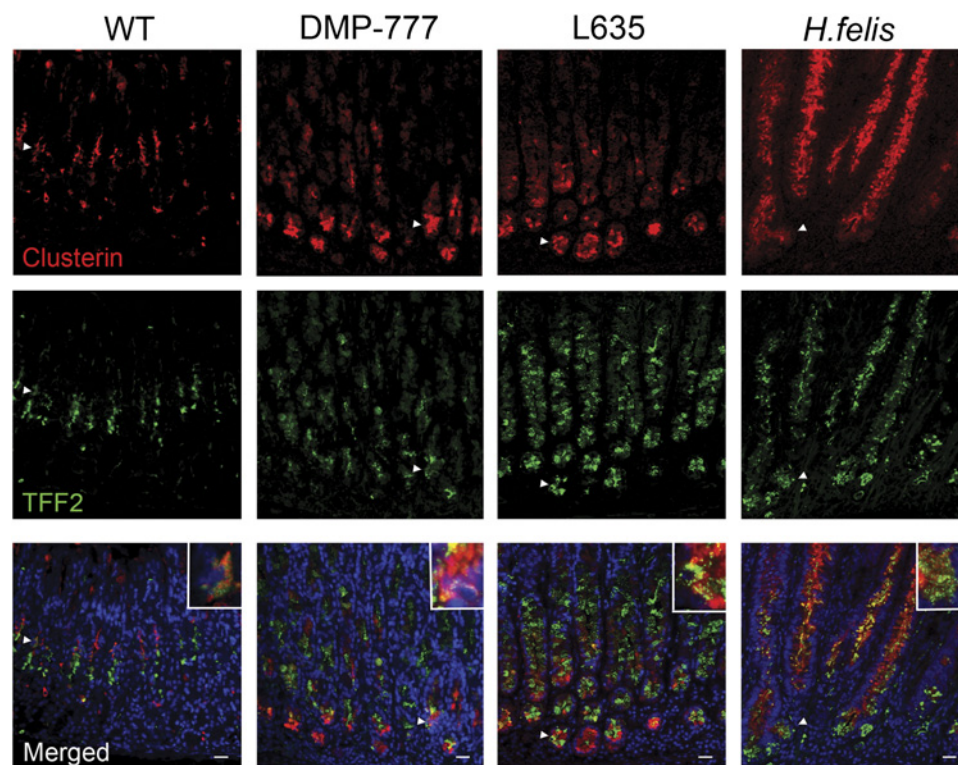
a prognostic biomarker. Clusterin staining was quantified by calculating the percentage of keratin-staining epithelial cells in each sample that were Clu positive (figure 5C and supplementary figure 8, available online only). There was a statistically significant association between the percentage of Clu-positive epithelial cells and stage. In particular, there were pairwise differences between all comparisons except stage 1 versus 3, and stage 3 versus 4 (figure 5D). Both positive Clu staining and stage were associated with survival (p values of 0.0232 and <0.0001, respectively). Clusterin was modelled using a restricted cubic spline with four knots. While the second knot (consisting of 23–43% Clu-positive epithelial staining) correlated with longer survival time, the 43–95% staining group was associated with shorter survival time (figure 5E). Furthermore, the model including both stage and percentage of Clu staining had a

Figure 2 Quantitative real-time PCR (qRT-PCR) assay of selected upregulated transcripts from each comparison category. Expression of selected upregulated transcripts from each category was assessed by qRT-PCR in RNA isolated from the whole fundic stomach (three mice per group). Pan-spasmodic polypeptide-expressing metaplasia (SPEM) (A) and acute SPEM (B) transcripts were associated with the emergence of SPEM, while SPEM with inflammation (C), specific to SPEM with inflammation (D), and SPEM with chronic inflammation (E) relate to the progression of SPEM lineages. Results are shown as fold change compared with the mean value of the control group (labelled WT). Single asterisks in A, B and C signify significant upregulation compared with wild type (WT). Double asterisks in D are significant compared with DMP-777-induced SPEM. Significance in E (+) is noted compared with 12-month *H felis* infection. All values are shown as means \pm SE of the mean, SE ($p < 0.05$ by Mann-Whitney U test). This figure is produced in colour in the online journal—please visit the website to view the colour figure.



Gastric cancer

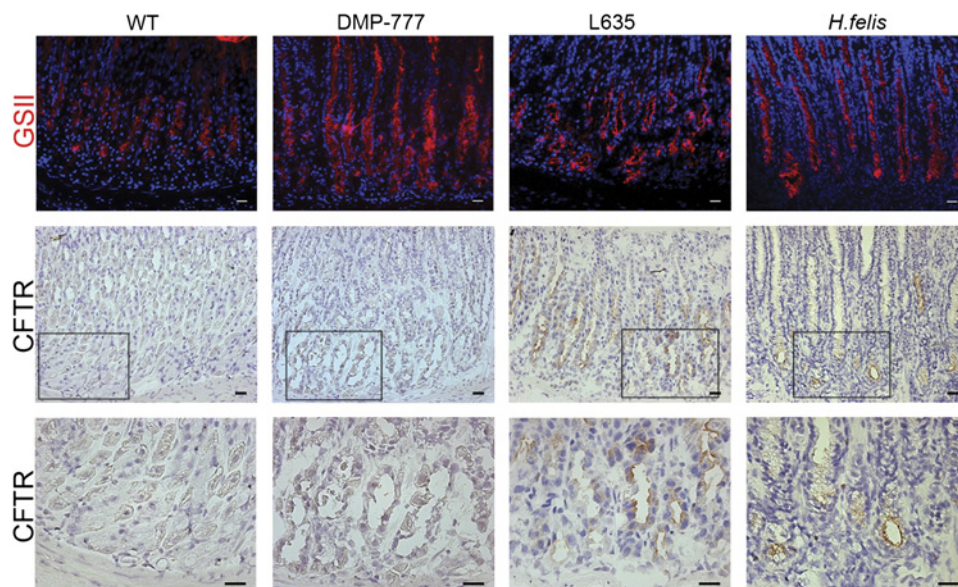
Figure 3 Expression of clusterin in normal murine gastric mucosa and spasmodic polypeptide-expressing metaplasia (SPEM) models. Sections of C57BL/6 mouse fundic mucosa were immunostained with antibodies against clusterin (top panels, red) and TFF2 (middle panels, green). In wild-type (WT) mice, clusterin was expressed in cells located in the isthmus and co-labelled with TFF2 in a small number of cells (arrowheads and higher magnification inset). Clusterin expression was detected throughout all SPEM lineages (14-day DMP-777 administration, 3-day L635 administration and 12-month *H felis* infection) (arrowheads and higher magnification insets). 4',6-diamidino-2-phenylindole (blue). Bar=20 μ m. This figure is produced in colour in the online journal—please visit the website to view the colour figure.



c-index of 0.86, which is equivalent to an area under the receiver operating characteristic curve (demonstrating good prediction).

CFTR expression was also investigated to understand the correlation between murine and human gastric metaplasias. Similar to murine expression patterns, CFTR was undetectable in normal gastric mucosa (figure 6). Conversely, CFTR was not observed in human SPEM even though it was accompanied by prominent inflammation. Nevertheless, intestinal metaplasia showed strong CFTR expression in the apical membranes throughout the glands. An analysis of CFTR expression in adenocarcinomas using tissue arrays was not possible because all available antibody reagents only perform well in frozen sections.

Figure 4 Expression of cystic fibrosis transmembrane conductance regulator (CFTR) in normal murine gastric mucosa and spasmodic polypeptide-expressing metaplasia (SPEM) models. Frozen sections of C57BL/6 mouse fundic mucosa were immunostained with either GSII lectin (a mucous neck cell and SPEM marker) or an antibody against CFTR to investigate CFTR protein expression in SPEM. Top panel: GSII (green) labels mucous neck cells in wild-type (WT) stomach mucosa and SPEM at the bases of glands in each of the SPEM models. Middle and bottom panels: Frozen sections immunohistochemical staining for CFTR showed no CFTR expression was detected in either WT mucosa or non-inflammatory SPEM (DMP-777-induced SPEM). The inset shows magnification of the bases of glands. CFTR expression was detected on the apical membranes of SPEM cells accompanied by inflammation (3-day L635 administration and 12-month *H felis* infection). Scale bars=20 μ m. This figure is produced in colour in the online journal—please visit the website to view the colour figure.



Nevertheless, taken together with the murine tissue data, these results suggest a correlation between SPEM with inflammation in mice and intestinal metaplasia in humans, supporting the hypothesis that murine SPEM with inflammation is more advanced and acquires intestinal characteristics.

DISCUSSION

Chronic *H pylori* infection in humans results in the loss of parietal cells accompanied by prominent inflammation. Our previous data have shown that parietal cell loss without inflammation (DMP-777 treatment) results in the transdifferentiation of chief cells into SPEM,⁵ possibly as a transient and local injury response

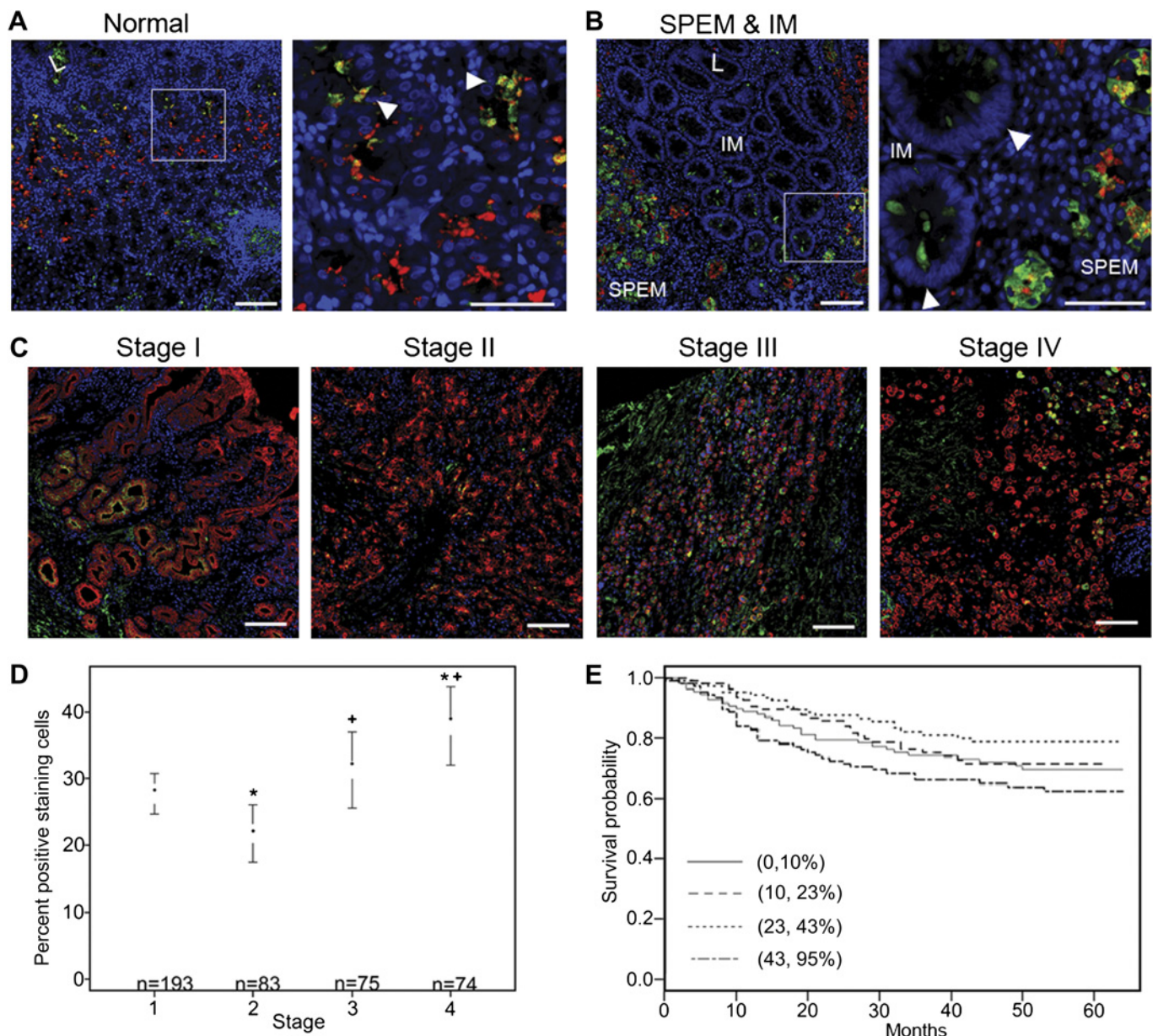


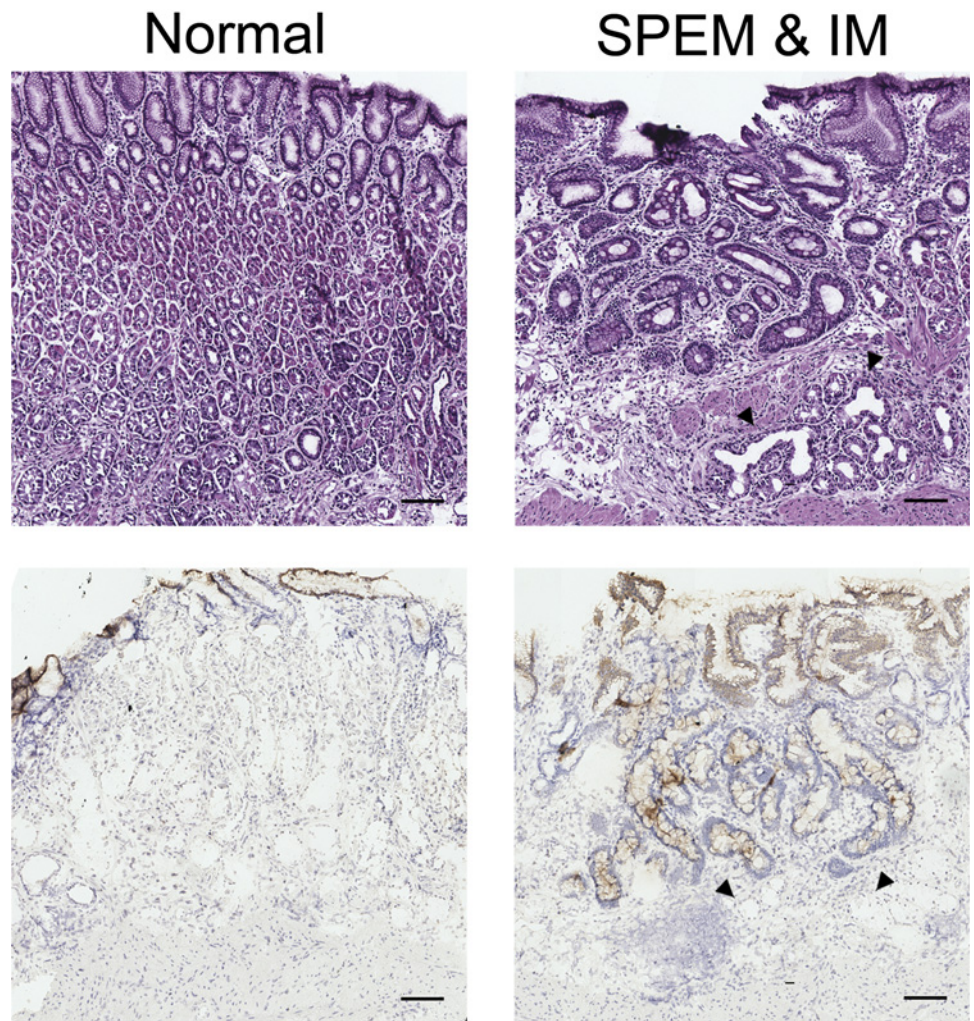
Figure 5 Clusterin expression in human normal gastric mucosa, metaplasia of the stomach and gastric cancer. (A) In normal glands, clusterin (green) was detected in the isthmus and in a few cells dual-labelled with TFF2 (red) as seen in the inset (arrowheads in top right panel). The sample shown was taken from the University of Tokyo metaplasia array. (B) Clusterin was prominently expressed throughout spasmodic polypeptide-expressing metaplasia (SPEM) glands as marked by TFF2 in red. In intestinal metaplasia (IM), clusterin was limited to a few cells at the base of glands (designated by arrowheads in bottom right panel). These staining patterns were found in 90% of SPEM samples and 45% of intestinal metaplasia samples on the University of Tokyo metaplasia tissue array. Left panel scale bar=100 μ m. Inset panel scale bar=50 μ m. (C) Representative images from a human gastric cancer tissue microarray show clusterin (green) expression in gastric cancer cells in each stage. Pan-cytokeratin staining (red) marks epithelial cells. Clusterin expression was present in all stages of cancer (I–IV) with averages of 27.75%, 21.82%, 31.32% and 37.94% clusterin-positive epithelial cells, respectively. 4',6-diamidino-2-phenylindole (blue). Bar=100 μ m. (D) The percentage of clusterin-positive epithelial cells was statistically significantly related to tumour stage by analysis of variance ($p=0.05$). There were significant differences in clusterin staining between stage 1 compared with stages 2 and 4 (labelled with *) and stage 2 versus stages 3 and 4 (labelled with +). (E) Estimated survival curves of clusterin by staining percentage categorised into four quartiles. The highest staining quartile (43–95% clusterin-positive epithelial cells) correlated with the worst survival outcome. This figure is produced in colour in the online journal—please visit the website to view the colour figure.

mechanism. However, when SPEM becomes chronic, under the continuing influence of chronic inflammation as in the setting of *H pylori* infection, SPEM progresses to dysplasia. Although SPEM alone is not sufficient for progression to dysplasia, it is necessary for the initiation of carcinogenesis. Therefore, metaplastic cell lineages such as SPEM and intestinal metaplasia are considered neoplastic precursors. Intestinal metaplasia arises in the presence of pre-existing SPEM^{2–4} suggesting a progression from SPEM to

intestinal metaplasia and then to neoplasia. A number of investigators have utilised chronic *H felis* infection in mice as a model for the development of metaplasia and dysplasia in the stomach.^{5–7} *H felis*-infected mice do not develop phenotypic intestinal metaplasia, but instead SPEM progresses directly to dysplasia.^{6–7} The present investigation indicates that, while phenotypic intestinal metaplasia may not develop from SPEM in *H felis*-infected mice, over time the SPEM lineages do begin to

Gastric cancer

Figure 6 Cystic fibrosis transmembrane conductance regulator (CFTR) expression in human normal gastric mucosa and in metaplasia of the human stomach. Frozen sections of human stomach were immunostained with an antibody against CFTR (bottom panels). Top panels are H&E staining of sections for orientation and morphology. CFTR was absent from normal mucosa (bottom left) and spasmodic polypeptide-expressing metaplasia (SPEM) lineages (designated by arrowheads in right panels). The diffuse cytoplasmic immunoreactivity seen in surface cells is non-specific as CFTR is localised to apical membranes. However, expression was observed in intestinal metaplasia (bottom right). Due to limitations of the CFTR antibody and the lack of availability of frozen adenocarcinoma samples, CFTR expression was not evaluated in cancers. Bar=100 μ m. This figure is produced in colour in the online journal—please visit the website to view the colour figure.



express intestinal transcripts, including CFTR and villin. Therefore, while these lineages may not display all of the characteristics of goblet cells and absorptive cells as in human intestinal metaplasia, they do represent further alterations towards more intestinal characteristics that correlate with susceptibility to the development of dysplasia (figure 1).

Studies using DMP-777 and L635 have shown that parietal cell loss is sufficient to induce SPEM, but the presence of inflammation is necessary for the progression of SPEM to a more proliferative metaplasia as well as to gastritis cystica profunda/dysplasia.^{5 8 24} In this study, we analysed the transcriptional expression of three SPEM models, establishing expression profiles for each lineage model. Specific comparisons of these profiles identified commonalities and differences among the SPEM lineages arising in different milieus. Thirteen transcripts were upregulated in two comparison categories (pan-SPEM and acute SPEM) indicative of SPEM initiation. Two of these, the secreted glycoprotein Wfdc2/HE4 and the poorly characterised ATPase Fig11, were previously reported as upregulated in SPEM from gastrin null mice after only 1 day of DMP-777 treatment.¹⁰ Another secreted glycoprotein, Clu, was also upregulated in SPEM. Similar to HE4, Clu was expressed in all SPEM lineages. A recent study has shown that Clu upregulation may be induced by gastrin,¹³ which is elevated in our mouse models of SPEM. However, Clu is also upregulated in SPEM from DMP-777-treated gastrin null mice (data not shown), indicating that gastrin-independent pathways exist for Clu upregulation.

Although the mechanisms for Clu upregulation are unclear, Clu represents a specific marker of SPEM induction in the gastric oxyntic mucosa.

Comparisons of expression profiles of the inflammatory SPEM models identified putative markers of advanced SPEM. In particular, prominent upregulation of CFTR was observed in both inflammatory SPEM models, but was undetectable in normal glands and in the non-inflammatory DMP-777-induced SPEM lineages. This represents the first definite expression difference among phenotypic SPEM lineages. Along with the other changes in intestinal transcripts such as villin, these findings suggest that inflammation elicits upregulation of genes, such as CFTR, which are more characteristic of the duodenum. As inflammation is required for progression of metaplasia to dysplasia, it follows that SPEM accompanied by prominent inflammation acquires intestinal markers. Moreover, Varon *et al*²² have suggested *Helicobacter*-induced metaplasia advances after 75 weeks to express Muc2, an intestinal metaplasia marker, in the upper portions of glands. The comparisons in the present study represent expression profiles that can be used to distinguish more advanced SPEM with intestinal characteristics (SPEM-IC), which is susceptible to progression to dysplasia. It remains unclear at this time whether proteins such as Clu and CFTR represent markers of the metaplastic process or whether they directly contribute to the progression of disease. Direct analysis of these questions remains problematical because there are no in-vitro models of normal chief cells and metaplastic

lineages (SPEM and intestinal metaplasia). Nevertheless, we anticipate that the rapid induction of metaplasia following L635 treatment will aid future examination of candidate protein influences using mouse strains with targeted gene disruption.

Taken together, the identification of differences among the expression profiles of phenotypic SPEM lineages illustrates the need to characterise in greater detail SPEM lineages found in the various models of metaplasia of the stomach and gastric cancer. Although SPEM was initially underappreciated as a preneoplastic lesion, recent investigations have illustrated the high prevalence of SPEM in numerous mouse models of gastric homeostasis and gastric cancer.^{25–30} The loss of *Klf4* in glandular tissues results in the development of a SPEM phenotype in the absence of inflammation.²⁶ Similar to DMP-777-induced SPEM, SPEM in *Klf4*-deficient mice does not acquire intestinal characteristics (such as *Muc2* or villin expression) nor does it progress to dysplasia. Keeley and Samuelson²⁵ and Jain *et al*²⁷ reported that the loss of *Hip1r* in parietal cells resulted in apoptotic loss of parietal cells and chief cells. A SPEM lineage accompanied by inflammatory infiltrates emerged at 5 weeks of age.^{25–27} Expression of intestinal features such as *Muc2* and villin is unknown in this SPEM model; however, this model is of interest for comparison with L635-induced SPEM (an acute SPEM model with inflammation). *K19-C2mE* transgenic mice, which overexpress COX-2 and microsomal prostaglandin E synthase-1 (mPGES-1), develop SPEM at 12 weeks of age and then progress to tumours at 48 weeks.²⁸ The addition of Wnt1 expression (*K19-Wnt1/C2mE* or *Gan* mice) resulted in SPEM at 5 weeks of age progressing to dysplastic tumours at 20 weeks.²⁹ In these models, the development of mucosal lesions was associated with prominent macrophage infiltrates similar to *H felis*-induced SPEM. In contrast to all SPEM models utilised in this study, mice deficient for *Runx3* develop a SPEM phenotype without prominent inflammation and without the loss of parietal cells. Although there is no inflammatory infiltrate, cells at the base of some SPEM glands expressed intestinal markers, *Muc2* and *CDX2*,³⁰ which are not seen in our metaplasia models. This model is of interest for comparison because of the progression of SPEM to acquire intestinal characteristics without the presence of inflammation or loss of parietal cells. The markers identified in our present investigations should provide reference points for analysis of the metaplastic lineages that arise in these other mouse models.

By establishing commonalities and differences in the expression patterns in our three murine SPEM models, we were able to find novel potential biomarkers of metaplasia in the human stomach. While all SPEM lineages in mice expressed *Clu*, we found that 90% of SPEM and 46% of intestinal metaplasia in humans expressed *Clu*. In human intestinal metaplasia, *Clu* localised to a few cells at the base of the intestinal metaplasia, which is the region suggested as a transitional and proliferative area of intestinal metaplasia arising from SPEM.⁴ Clusterin may be acting in an anti-apoptotic or cytoprotective manner to help maintain this transitional niche. Clusterin upregulation was maintained in the majority of intestinal-type and diffuse-type cancers. Correlation between *Clu* expression and stage was U-shaped, suggesting *Clu* functions differently in the different stages of cancer, a pattern previously observed in other types of cancers.³¹ Adverse patient outcome was associated with the highest percentage of *Clu* expression, which was more frequently seen in late-stage cancers. This study supports the recent findings that high *Clu* expression in late-stage gastric cancers correlated with a poor outcome.³² Therefore, *Clu* is a useful biomarker for SPEM and an adverse prognostic marker

for adenocarcinomas. Conversely, CFTR expression was absent in human SPEM, but was upregulated in intestinal metaplasia. These findings show that expression profiles in murine SPEM with inflammation (SPEM–IC) overlap with human intestinal metaplasia, suggesting that SPEM–IC is a more advanced SPEM lineage (figure 1). Further investigation of murine SPEM lineages will provide greater insight into the heterogeneity of SPEM as well as the progression of early stage SPEM to SPEM–IC in mouse and, by analogy, to the progression of SPEM to intestinal metaplasia in humans.

In summary, we have established distinct expression profiles of SPEM with or without inflammation that illustrate similarities among all SPEM lineages and differences in SPEM lineages with the potential for progression to dysplasia in mice. From these profiles, *Clu* upregulation was verified as a biomarker of SPEM and poor patient outcome. In addition, CFTR was identified as a biomarker of SPEM with inflammation in mice and intestinal metaplasia in humans. The expression profiles of SPEM lineages with inflammation, especially *H felis* infection-induced SPEM, identified a more advanced SPEM lineage in mice that has adopted some intestinal characteristics. These studies support a model of metaplastic progression in mice that begins with the induction of SPEM and advances to SPEM–IC that may have dysplastic potential. The studies also indicate that the mouse model of chronic *H felis* infection does mimic the analogous human condition of *H pylori* infection, suggesting a progression of parietal cell loss to the initiation of SPEM to further metaplastic progression towards intestinalising metaplasia in the presence of inflammatory influences.

Acknowledgements The authors would like to thank Dr Joseph Roland for artistic contributions.

Contributors VGW performed experiments, analysed data, prepared figures and wrote the manuscript. JFS performed experiments, analysed data and edited the manuscript. BJL performed statistical analysis and edited the manuscript. KTN performed experiments and edited the manuscript. JAW developed a new system for analysis of array staining. PEF synthesised L635 and edited the manuscript. NAA developed CFTR antibodies and analysed data. JGF supervised *Helicobacter* infections studies, developed experimental design and edited the manuscript. JRG developed experimental design, analysed data and edited the manuscript.

Funding These studies were supported by grants from a Department of Veterans Affairs merit review award, NIH grant R01 DK071590, and an ARRA supplement (DK071590-S1) (to JRG); NIH grants R01 AI037750 and P30 ES02109 (to JGF); R01 DK 077065 (to NAA); P50 CA95060 (to BJL). This work was supported by core resources of the Vanderbilt Digestive Disease Center (P30 DK058404) and the Vanderbilt–Ingram Cancer Center, and imaging was supported by both the Vanderbilt combined imaging shared resource and the shared imaging resource of the Vanderbilt Epithelial Biology Center.

Competing interests None.

Ethics approval Ethics approval was provided by Vanderbilt institutional review board.

Provenance and peer review Not commissioned; externally peer reviewed.

REFERENCES

- Blaser M, Parsonnet J. Parasitism by the 'slow' bacterium *Helicobacter pylori* leads to altered gastric homeostasis and neoplasia. *J Clin Invest* 1994;**94**:4–8.
- Yoshizawa N, Takenaka Y, Yamaguchi H, *et al*. Emergence of spasmodic polypeptide-expressing metaplasia in Mongolian gerbils infected with *Helicobacter pylori*. *Lab Invest* 2007;**87**:1265–76.
- Nam KT, Lee HJ, Mok H, *et al*. Amphiregulin-deficient mice develop spasmodic polypeptide-expressing metaplasia and intestinal metaplasia. *Gastroenterology* 2009;**136**:1288–96.
- Goldenring JR, Nam KT, Wang TC, *et al*. Spasmodic polypeptide-expressing metaplasia and intestinal metaplasia: time for reevaluation of metaplasias and the origins of gastric cancer. *Gastroenterology* 2010;**138**:2207–10; 2210.e1.
- Nam KT, Lee HJ, Sousa JF, *et al*. Mature chief cells are cryptic progenitors for metaplasia in the stomach. *Gastroenterology* 2010;**139**:2028–37.e9.

Gastric cancer

6. **Wang TC**, Dangler CA, Chen D, *et al*. Synergistic interaction between hypergastrinemia and *Helicobacter* infection in a mouse model of gastric cancer. *Gastroenterology* 2000;**118**:36–47.
7. **Houghton J**, Stoicov C, Nomura S, *et al*. Gastric cancer originating from bone marrow-derived cells. *Science* 2004;**306**:1568–71.
8. **Goldring JR**, Ray GS, Coffey RJ, *et al*. Reversible drug-induced oxyntic atrophy in rats. *Gastroenterology* 2000;**118**:1080–93.
9. **Nomura S**, Yamaguchi H, Ogawa M, *et al*. Alterations in gastric mucosal lineages induced by acute oxyntic atrophy in wild type and gastrin deficient mice. *Am J Physiol Gastrointest Liver Physiol* 2004;**288**:G362–75.
10. **Nozaki K**, Ogawa M, Williams JA, *et al*. A molecular signature of gastric metaplasia arising in response to acute parietal cell loss. *Gastroenterology* 2008;**134**:511–21.
11. **Lee HJ**, Nam KT, Park HS, *et al*. Gene expression profiling of metaplastic lineages identifies CDH17 as a prognostic marker in early stage gastric cancer. *Gastroenterology* 2010;**139**:213–25.e3.
12. **Oshima M**, Oshima H, Matsunaga A, *et al*. Hyperplastic gastric tumors with spasmodic polypeptide-expressing metaplasia caused by tumor necrosis factor- α -dependent inflammation in cyclooxygenase-2/microsomal prostaglandin E synthase-1 transgenic mice. *Cancer Res* 2005;**65**:9147–51.
13. **Fjeldbo CS**, Bakke I, Erlandsen SE, *et al*. Gastrin upregulates the prosurvival factor secretory clusterin in adenocarcinoma cells and in oxyntic mucosa of hypergastrinemic rats. *Am J Physiol Gastrointest Liver Physiol* 2012;**302**:G21–33.
14. **Collard MW**, Griswold MD. Biosynthesis and molecular cloning of sulfated glycoprotein 2 secreted by rat Sertoli cells. *Biochemistry* 1987;**26**:3297–303.
15. **McLaughlin L**, Zhu G, Mistry M, *et al*. Apolipoprotein J/clusterin limits the severity of murine autoimmune myocarditis. *J Clin Invest* 2000;**106**:1105–13.
16. **Aronow BJ**, Lund SD, Brown TL, *et al*. Apolipoprotein J expression at fluid-tissue interfaces: potential role in barrier cytoprotection. *Proc Natl Acad Sci U S A* 1993;**90**:725–9.
17. **Ahuja HS**, Tenniswood M, Lockshin R, *et al*. Expression of clusterin in cell differentiation and cell death. *Biochem Cell Biol* 1994;**72**:523–30.
18. **Lee S**, Hong SW, Min BH, *et al*. Essential role of clusterin in pancreas regeneration. *Dev Dyn* 2011;**240**:605–15.
19. **Ameen N**, Alexis J, Salas P. Cellular localization of the cystic fibrosis transmembrane conductance regulator in mouse intestinal tract. *Histochem Cell Biol* 2000;**114**:69–75.
20. **McDaniel N**, Pace AJ, Spiegel S, *et al*. Role of Na-K-2Cl cotransporter-1 in gastric secretion of nonacidic fluid and pepsinogen. *Am J Physiol Gastrointest Liver Physiol* 2005;**289**:G550–60.
21. **Lee A**, Fox JG, Otto G, *et al*. A small animal model of human *Helicobacter pylori* active chronic gastritis. *Gastroenterology* 1990;**99**:1315–23.
22. **Varon C**, Dubus P, Mazurier F, *et al*. *Helicobacter pylori* infection recruits bone marrow-derived cells that participate in gastric preneoplasia in mice. *Gastroenterology* 2012;**142**:281–91.
23. **Oshima H**, Hioki K, Popivanova BK, *et al*. Prostaglandin E signaling and bacterial infection recruit tumor-promoting macrophages to mouse gastric tumors. *Gastroenterology* 2011;**140**:596–607.e7.
24. **Fox JG**, Blanco M, Murphy JC, *et al*. Local and systemic immune responses in murine *Helicobacter felis* active chronic gastritis. *Infect Immun* 1993;**61**:2309–15.
25. **Keeley TM**, Samuelson LC. Cytodifferentiation of the postnatal mouse stomach in normal and Huntingtin-interacting protein 1-related-deficient mice. *Am J Physiol Gastrointest Liver Physiol* 2010;**299**:G1241–51.
26. **Katz JP**, Perreault N, Goldstein BG, *et al*. Loss of Klf4 in mice causes altered proliferation and differentiation and precancerous changes in the adult stomach. *Gastroenterology* 2005;**128**:935–45.
27. **Jain RN**, Al-Menhali AA, Keeley TM, *et al*. Hip1r is expressed in gastric parietal cells and is required for tubulovesicle formation and cell survival in mice. *J Clin Invest* 2008;**118**:2459–70.
28. **Oshima H**, Oshima M, Inaba K, *et al*. Hyperplastic gastric tumors induced by activated macrophages in COX-2/mPGES-1 transgenic mice. *EMBO J* 2004;**23**:1669–78.
29. **Oshima H**, Matsunaga A, Fujimura T, *et al*. Carcinogenesis in mouse stomach by simultaneous activation of the Wnt signaling and prostaglandin E2 pathway. *Gastroenterology* 2006;**131**:1086–95.
30. **Ito K**, Chuang LS, Ito T, *et al*. Loss of Runx3 is a key event in inducing precancerous state of the stomach. *Gastroenterology* 2011;**140**:1536–46.e8.
31. **Rizzi F**, Bettuzzi S. The clusterin paradigm in prostate and breast carcinogenesis. *Endocr Relat Cancer* 2010;**17**:R1–17.
32. **Bi J**, Guo AL, Lai YR, *et al*. Overexpression of clusterin correlates with tumor progression, metastasis in gastric cancer: a study on tissue microarrays. *Neoplasia* 2010;**57**:191–7.



Heterogeneity in mouse spasmodic polypeptide-expressing metaplasia lineages identifies markers of metaplastic progression

Victoria G Weis, Josane F Sousa, Bonnie J LaFleur, et al.

Gut published online July 7, 2012
doi: 10.1136/gutjnl-2012-302401

Updated information and services can be found at:
<http://gut.bmj.com/content/early/2012/07/06/gutjnl-2012-302401.full.html>

These include:

Data Supplement

"Supplementary Data"
<http://gut.bmj.com/content/suppl/2012/07/06/gutjnl-2012-302401.DC1.html>

References

This article cites 32 articles, 8 of which can be accessed free at:
<http://gut.bmj.com/content/early/2012/07/06/gutjnl-2012-302401.full.html#ref-list-1>

P<P

Published online July 7, 2012 in advance of the print journal.

Email alerting service

Receive free email alerts when new articles cite this article. Sign up in the box at the top right corner of the online article.

Topic Collections

Articles on similar topics can be found in the following collections

[Pancreatic cancer](#) (558 articles)
[Pancreas and biliary tract](#) (1737 articles)

Advance online articles have been peer reviewed, accepted for publication, edited and typeset, but have not yet appeared in the paper journal. Advance online articles are citable and establish publication priority; they are indexed by PubMed from initial publication. Citations to Advance online articles must include the digital object identifier (DOIs) and date of initial publication.

To request permissions go to:
<http://group.bmj.com/group/rights-licensing/permissions>

To order reprints go to:
<http://journals.bmj.com/cgi/reprintform>

To subscribe to BMJ go to:
<http://group.bmj.com/subscribe/>

Notes

Advance online articles have been peer reviewed, accepted for publication, edited and typeset, but have not yet appeared in the paper journal. Advance online articles are citable and establish publication priority; they are indexed by PubMed from initial publication. Citations to Advance online articles must include the digital object identifier (DOIs) and date of initial publication.

To request permissions go to:

<http://group.bmj.com/group/rights-licensing/permissions>

To order reprints go to:

<http://journals.bmj.com/cgi/reprintform>

To subscribe to BMJ go to:

<http://group.bmj.com/subscribe/>